

RESEARCH ARTICLE

Modelling and Calculation of Characteristic Parameters of the Active and Buffer Layers in Organic Solar Cell

Minh Duc Tran and Nguyen Dinh Lam*

Faculty of Engineering Physics and nanotechnology, VNU-University of Engineering and Technology, Vietnam National University, 144, Xuanthuy, Caugiay, Hanoi, Vietnam

Abstract: Background: The active layer not only must have a strong light absorption in the visible spectrum but must also be sufficient for charge carrier transport to the electrodes. Electrons in conducting polymer transport by hopping between different energy levels resulted in much lower charge mobility. Therefore, the thickness of the active layer must be limited, so the separated charge can reach the corresponding electrodes without recombination. However, a thin active layer has weaker light absorption, resulting in the low photogenerated current in organic solar cell devices. Furthermore, buffer layers usually have high charge mobility, which in turn would enhance the transportation of charge from the active layer to electrodes. Metal oxides have been studied to be used as a cathode buffer layer, such as titanium dioxide (TiO₂), zinc oxide (ZnO), etc.

ARTICLE HISTORY

Received: August 30, 2019
Revised: November 04, 2019
Accepted: February 03, 2020

DOI:
10.2174/1573413716666200217103420

Objective: In this work, behaviors of the photon-electrical characteristics with variation in thickness of the active (poly(3-hexylthiophene-2,5-diyl) and phenyl-C61 butyric acid methyl ester blend) and buffer (zinc oxide) layers were investigated.

Method: The influences of the thickness of the active and buffer layers on characteristic parameters of organic solar cells were investigated by solving the drift and diffusion equation with the photo-generated current given by the Hetch equation.

Results: The optimum thickness was obtained around 100 nm and below 10 nm for the active and the ZnO buffer layers, respectively.

Conclusion: Thinner active layer resulted in lower photocurrent due to poor light absorption while at 150 nm thick and above, PCE of the device reduced rapidly because of the high recombination rate of photogenerated electron-hole pairs. ZnO buffer layer was used as an electron transport layer and a hole blocking layer in order to improve the cell's performance. The addition of ZnO enhanced the PCE up to 2.48 times higher than the conventional device.

Keywords: P3HT:PCBM, solar cell, ZnO buffer layer, thickness, active layer, electron transport layer.

1. INTRODUCTION

Organic solar cells (OSCs) based on the composition of conducting polymer and fullerene derivatives have drawn much attention. Owing to its advantages in the production cost and flexibility over conventional silicon-based devices, intensive research has been made in order to improve the power conversion efficiency (PCE) of these devices. Among the materials, poly(3-hexylthiophene-2,5-diyl) (P3HT) and phenyl-C61 butyric acid methyl ester (PCBM) have been the best-seller for more than a decade [1]. Aside from experimental research, theoretical works and simulation models

were also discussed to study further about the behavior of organic devices [2, 3]. For a conventional Si-based solar cell, the J – V characteristic under illumination was given by the following Eq. (1):

$$J = J_0 \left\{ \exp \left[\frac{q(V - JR_S)}{nkT} \right] - 1 \right\} + \frac{V - JR_S}{R_{sh}} - J_{sc} \quad (1)$$

where J_0 is the reverse saturation current density, n is the ideality factor, V is the applied voltage, R_S and R_{sh} are the series and shunt resistances, respectively. J_{sc} is the short circuit current density and also considered as the photocurrent. Even though the principles are quite similar, the nature of OSCs is quite different from its inorganic counterparts. For example, the behaviors of dark and illuminated current in an OSC are different from those in a Si-based device. Along with many factors, these are the reasons why Eq. (1) is no longer valid for an organic model. Furthermore, the

*Address correspondence to this author at the Faculty of Engineering Physics and nanotechnology, VNU-University of Engineering and Technology, Vietnam National University, 144, Xuanthuy, Caugiay, Hanoi, Vietnam; Tel: +84 902 233 144; E-mail: lamnd2005@gmail.com

mentioned model does not take the effect of the built-in potential V_{bi} into consideration. In OSCs, V_{bi} can be as large as 1.3 eV. Therefore, the effect of V_{bi} cannot be overlooked. By solving the continuity equation, Kumar *et al.* successfully modeled the J – V characteristic of the bulk heterojunction (BHJ) solar cells structure of ITO/PEDOT:PSS/P3HT:PCBM/Al and studied the influence of the constant electric field on the dark and illuminated current of the device [4]. The continuity equation is given by (Eq. 2):

$$J = q\mu n(x)F(x) + qD_n \frac{\partial n(x)}{\partial x} \quad (2)$$

where μ is the electron mobility, D_n is the electron diffusion coefficient, $F(x)$ is the electric field and $n(x)$ is the electron density. However, influences of thickness of the active layer were not still mentioned. Based on the same model for the dark current, a different attempt was made to simulate the photogenerated current in this paper. Then, the thickness of the active layer was varied to investigate its effect on the performance of the OSC devices. The active layer not only must have a strong light absorption in the visible spectrum but must also be sufficient for charge carrier transport to the electrodes. Electrons in conducting polymer transport by hopping between different energy levels resulted in much lower charge mobility ($\sim 10^{-7}$ – 10^{-1} cm²/V.s compared to $\sim 10^3$ cm²/V.s in inorganic semiconductor [5]). Therefore, the thickness of the active layer must be limited, so the separated charge can reach the corresponding electrodes without recombination. However, a thin active layer has weaker light absorption, resulting in the low photogenerated current in OSC devices. To achieve high power conversion efficiency (PCE), a compromise between absorption and recombination is required. For the blend of P3HT and PCBM, the optimum thickness of the active layer was reported to be 100 nm [1, 6, 7].

Beside optimizing the thickness of the active layer, the structure of the OSC device itself has also been innovated to increase cell efficiency. In the multi-layer BHJ structure, buffer layers (BLs) were introduced between the active layer and the electrode. These BLs usually have high charge mobility, which in turn would enhance the transportation of charge from the active layer to electrodes. For years, metal oxides have been studied to be used as a cathode buffer layer (CBL) such as titanium dioxide (TiO₂), zinc oxide (ZnO), *etc.* Among those, ZnO is the most widely used material, mainly due to its high electron mobility, high transmittance in the visible spectrum, low cost, simple fabrication process and environmental stability [8-11]. Moreover, the energy level position of ZnO material allows it to function well as both the electron transport layer (ETL) and the hole blocking layer (HBL) [12]. The influences of the ZnO buffer layer were also studied in this work by varied its thickness from 0 to 70 nm. The results indicated that the addition of ZnO buffer layer significantly improved the PCE of the device up to 24.8% compared to that of the device without the ZnO buffer layer.

2. METHODS

In this work, charges were assumed to travelled in one dimension to simplify the model. Details on the solution of Eq.(2) can be found in the work of Kumar *et al.* [4]. The final result, from which the drift and diffusion components

of the current in a practical diode can be calculated, is given by (Eq. 3):

$$J = \frac{qD_n N_c (V_{bi} - V + JR_s) \exp\left(\frac{-\Phi}{nkT}\right) \exp\left\{\exp\left[\frac{q(V - JR_s)}{nkT}\right] - 1\right\}}{dn \left\{1 - \exp\left[\frac{-q(V_{bi} - V + JR_s)}{nkT}\right]\right\}} + \frac{V - JR_s}{R_{sh}} \quad (3)$$

where N_c is the effective density of states, Φ is the electron injection barrier at the anode, d is the thickness of the active layer, R_s and R_{sh} is series and shunt resistance, respectively. To obtain the current density under illumination, the photocurrent (J_{ph}) was added to the model. J_{ph} , as a function of the applied field, was generated from the Hetch model for photocurrent [13], given by (Eq. 4):

$$J_{ph} = -2q\bar{G}\mu\tau \frac{V_{bi} - V}{d} \left\{1 - \exp\left[\frac{-d^2}{2\mu\tau(V_{bi} - V)}\right]\right\} \quad (4)$$

Holes and electrons were assumed to have the same mobility; hence the only product of $\mu\tau$ in the model with τ is the average lifetime of carriers with \bar{G} which is the averaged generation rate.

The structure of the organic solar cell in this work from top to bottom is ITO/ZnO/P3HT:PCBM/PEDOT:PSS/Ag. In that, the ITO layer plays as a cathode, to which electron will move after dissociation. The ZnO layer is the cathode buffer layer (CBL) or hole blocking layer (HBL) or electron transporting layer (ETL). The P3HT:PCBM layer is the optically active layer. The PEDOT:PSS layer is a polymer mixture that plays the role of the anode buffer layer (ABL) or electron blocking layer (EBL) or hole transport layer (HTL) has a band gap of 1.6 eV. The last layer -silver (Ag)- is used as an anode.

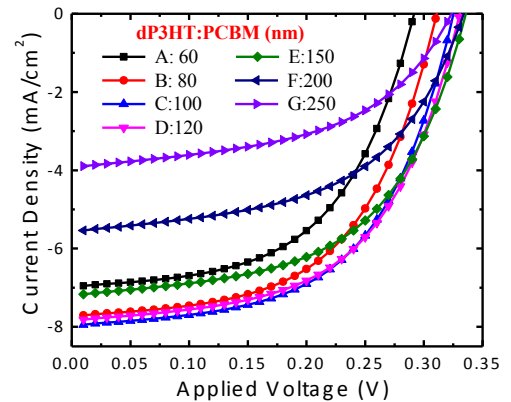


Fig. (1). The J – V characteristic of OSCs with variation in the thickness of active layer. (A higher resolution / colour version of this figure is available in the electronic copy of the article).

3. RESULTS AND DISCUSSION

For all simulated devices in this study, the energy level for corresponding materials, the thickness of the active layer and the ZnO buffer layer were adjusted. Other components were fixed for all calculations. Firstly, the device structure without the ZnO buffer layer was modeled and its active layer was varied from 60 to 250 nm, corresponded to device A to F. The J-V characteristics of these devices were shown in Fig. (1). The J_{sc} , FF, V_{oc} , and PCE values for each thick-

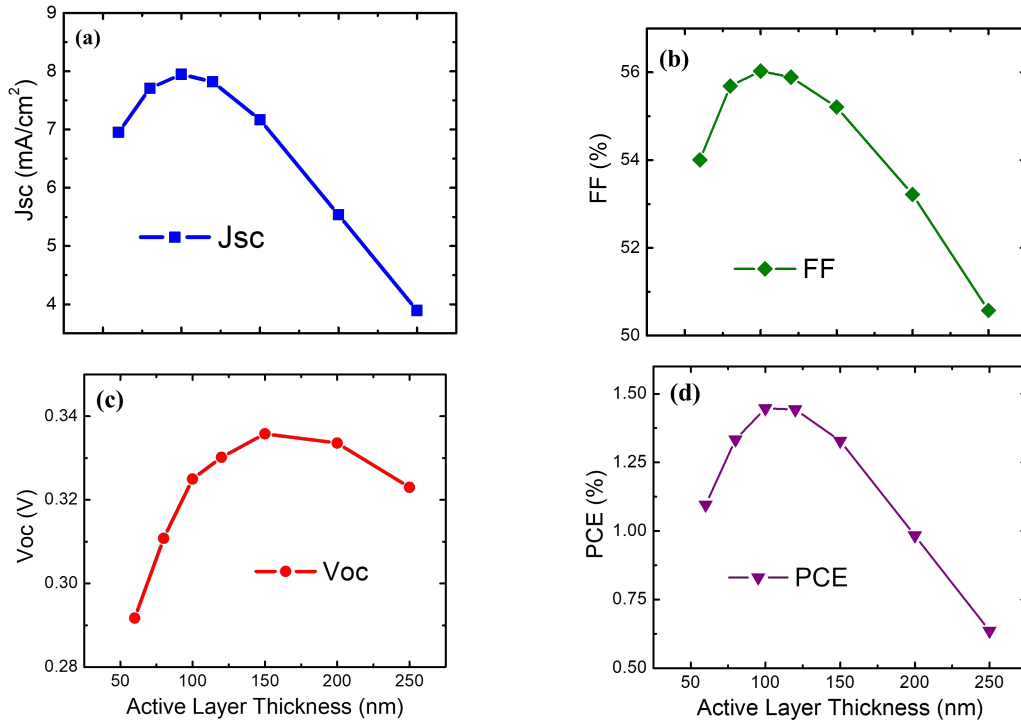


Fig. (2). Performance parameters of OSCs extracted from J-V curves with variation in the thickness of active layer. (A higher resolution / colour version of this figure is available in the electronic copy of the article).

ness of the active layer were extracted from J-V curves and depicted in Fig. (2). Due to poor absorption of the thin active layer, the J_{SC} of devices A and B were relatively low, at 6.95 and 7.71 mA/cm², respectively. This contributed to the low PCE, at 1.1% for device A and 1.3% for device B. The best performance was found at 100 nm thick of active layer (device C) and a minor decrease was seen in device D, at 120 nm thick of an active layer. The PCE of these thicknesses was 1.45% and 1.44%, respectively. However, the performance of the device rapidly reduced with the increase of thickness of the active layer. J_{SC} gradually decreased from 7.17 mA/cm² in device E to 3.89 mA/cm² in device G. This trend of reduction was also seen in the FF. Although the thick active layer benefits the absorption of photon due to the increase in generation rate, given by (Eq. 5):

$$G = \sum_0^d \alpha(\lambda)\Phi(\lambda)e^{-\alpha d} \quad (5)$$

with the absorption coefficient $\alpha(\lambda)$ and the photon flux $\Phi(\lambda)$, this is not comparable to the change in $(V_{bi} - V)/d$ in the Hetch model, hence the reduction of J_{ph} in thick active layer devices. From device E to G, V_{OC} and PCE decreased from 0.36 V to 0.32 V, and from 1.33 % to 0.64 %, respectively. Previous works reported that as the active layer thickness increased, the recombination rate became more and more significant, resulting in the loss of charges, which yields the reduction of J_{SC} and V_{OC}[7, 14, 15]. Overall, the 100 nm P3HT:PCBM active layer was found to deliver the best performance and this thickness would be used as a standard for the following study about the influences of the ZnO buffer layer.

For further investigation of the influences of the active layer thickness on the OSC current density, based on the

Eqs.(4, 5) and the experimental optical absorption spectra of the active layer, as shown in Fig. (3), the induced photon to current densities were calculated and depicted in Fig. (4). The results indicated that the OSCs optical absorption and induced photon to current density were in the range of photon wavelengths from 300 nm to 640 nm. The induced photon to current density got the highest value when the active layer was 100 nm in thick. This is satisfied with the best short circuit current density obtained by the J-V curves shown in Fig. (1).

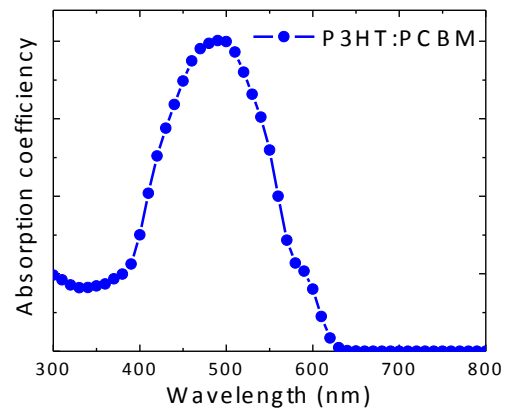


Fig. (3). Optical absorption spectrum of the active layer. (A higher resolution / colour version of this figure is available in the electronic copy of the article).

Fig. (5) presents the J – V characteristics of devices with the variation in thicknesses of the ZnO buffer layers. The appearance of ZnO film largely enhanced all parameters of the devices. The enhanced absorption of the ZnO layer re-

sulting in the increased J_{SC} from 7.95 mA/cm^2 of device A to 9.14 mA/cm^2 of device B. It was noticed that at the ZnO/PCBM interface, there exists a small difference between conduction band energy levels E_C of ZnO and PCBM. However, their valence band energy levels E_V have a much larger barrier. This means that electrons from the active layer can diffuse into the ZnO layer much easier than holes can. And since the presence of holes in the ZnO layer is little compared to electrons, the recombination rate can be largely reduced [16]. The large energy barrier from the addition ZnO can also raise the internal field intensity in the device, hence increasing the V_{OC} [9, 17-19]. In the simulation, the V_{OC} enhanced from 0.325 V to 0.58 V with the appearance of the ZnO buffer layer. Consequently, the PCE increased significantly from 1.45% to 3.6% . The influences of different thicknesses of the ZnO buffer layer on OSC characteristics were extracted from J-V curves and shown in Fig. (6a-6d). The highest J_{SC} value of 9.15 mA/cm^2 can be obtained by an 8 nm thick of the ZnO buffer layer (device C). As can be seen from (Fig. 6a), J_{SC} of the device will be clearly reduced as an increase of the thickness of the ZnO buffer layer. Due to its large band gap, the ZnO film only absorbs the UV spectrum of the solar irradiance. This resulted in a small increment of the charge generation rate and was immediately overwhelmed by the large recombination as the thickness increased. The reduction of J_{SC} was followed by FF, which is introduced in Fig. (6b). The J_0 can be extracted from the J – V characteristic of the device in the dark by fitting the data into the simplified Shockley Eq. (6):

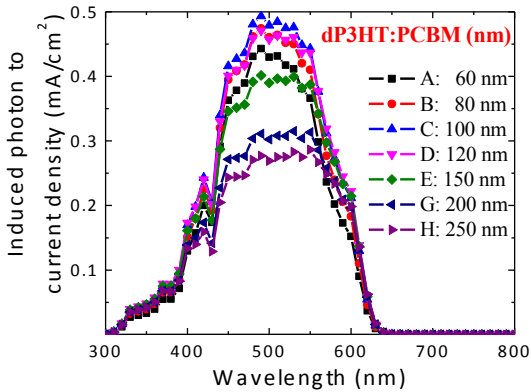


Fig. (4). Induced photon to current density with variation in the active layer thickness. (A higher resolution / colour version of this figure is available in the electronic copy of the article).

$$V_{OC} = \frac{nk_B T}{q} \ln \left(\frac{J_{SC}}{J_0} \right) \quad (6)$$

From Eq.(6) and V_{OC} from the simulation results, J_0 was found to decrease at a higher thickness of the ZnO layer. However, this decrement was much smaller than the reduction of J_{SC} . Therefore, the result of $\ln(J_{SC}/J_0)$ in these cases increased, yielded the increment of 2% in V_{OC} , as presented in Fig. (6c). However, an increment of V_{OC} could not compensate for the drop of FF, as this parameter reduced linearly from 69% to 65% . Overall, the optimum thickness for ZnO films was under 10 nm .

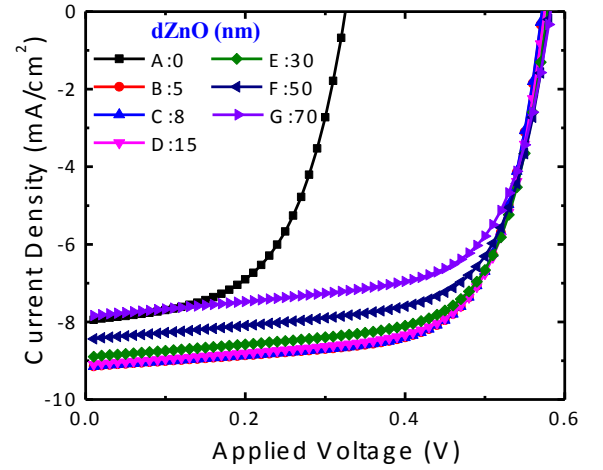


Fig. (5). The J – V characteristic of OSCs with variation in the thickness of ZnO buffer layer. (A higher resolution / colour version of this figure is available in the electronic copy of the article).

To further evaluate the quality of the results, we applied the simulation model to the work of Liang *et al.* [20] and recalculated the J – V characteristic of 4 devices with the ZnO films at approximately $4, 7, 20$ and 35 nm thick. The ZnO layer thickness, R_S and R_{sh} for each calculation were set, according to the original paper, while other parameters remained unchanged. Details on the result of the simulation are listed in Table 1. Overall, differences in J_{SC} and V_{OC} are negligible, at roughly about 0.12 mA/cm^2 and 0.01 V , respectively. However, for FF and PCE, it is quite noticeable. At 7 nm thick, the FF obtained from simulation is 2.13% larger than one from [20]. PCE from the simulation is also higher, at 3.42% compared to 3.30% . To explain the differences between these results, the role of the ideality factor n is investigated. In ideal cases, n is equal to 1 and this parameter is used to determine the quality of the diode. As the recombination is thickness dependent, n is expected to be different with each thickness[21]. But, since the study [20] did not mention this parameter, n remained unchanged in the simulation. This could be one reason for the mixed results of the 7 nm model. Regarded, the simulation model still exhibits acceptable results with the experimental data in terms of optimum thickness.

CONCLUSION

In summary, the J – V characteristic of an organic solar cell has been modeled. By using the Hetch model for photocurrent, in addition to solving the drift and diffusion equation of electron in a semiconductor, the influences of active layer thickness and ZnO buffer layer thickness on the device performance have successfully studied. For the active layer, the result showed that the optimum thickness is around 100 nm . The thinner layer resulted in lower photocurrent due to poor light absorption while at 150 nm thick and above, PCE of the device reduced rapidly because of the high recombination rate of photogenerated electron-hole pairs. ZnO layer was used as an electron transport layer and a hole blocking layer in order to improve the cell's performance. The addition of ZnO enhanced the PCE up to 2.48 times higher than the conventional device. However, as its thickness increased, the FF

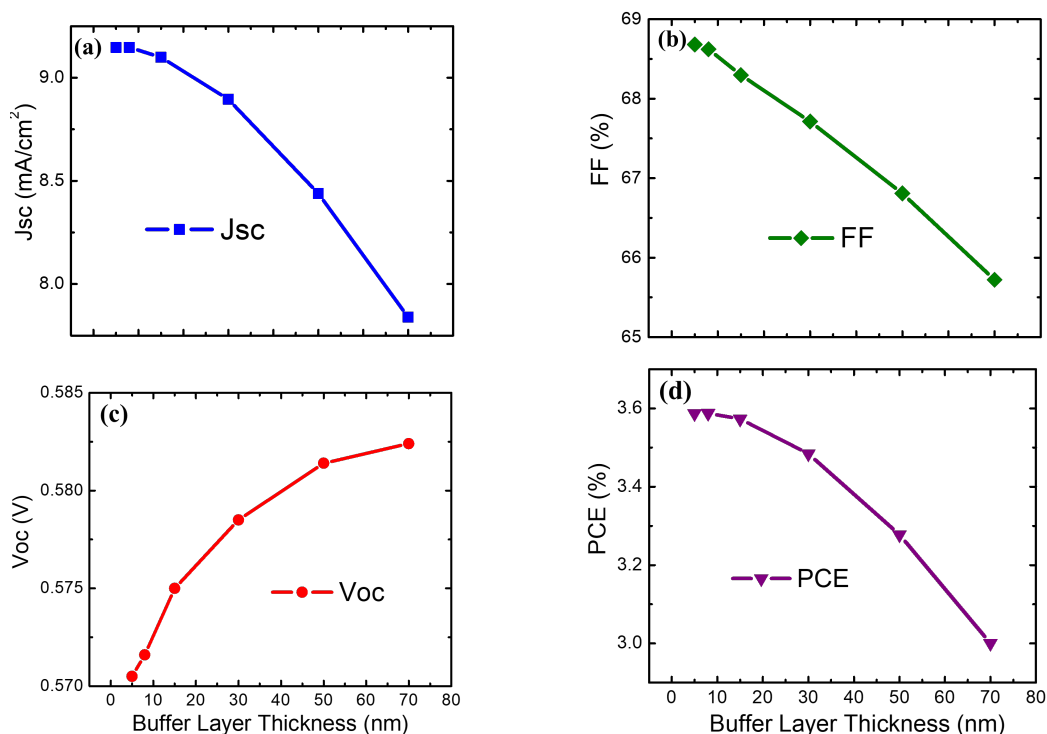


Fig. (6). Performance parameters of OSCs extracted from J-V curves with variation in the thickness of ZnO buffer layer. (A higher resolution / colour version of this figure is available in the electronic copy of the article).

Table 1. Comparison parameters of OSCs between ref. 14 and simulation data results.

ZnO Thickness (nm)	J _{sc} (mA/cm ²)		V _{oc} (V)		FF (%)		PCE (%)	
	Ref. 14	Simulation	Ref. 14	Simulation	Ref. 14	Simulation	Ref. 14	Simulation
4	9.17	9.05	0.60	0.61	52	51.85	2.90	2.86
7	9.59	9.52	0.61	0.618	56	58.13	3.30	3.42
20	9.48	9.478	0.61	0.615	51	52.61	2.99	3.07
35	9.42	9.374	0.61	0.6115	51	50.62	2.94	2.9

reduced gradually by the loss of charges due to recombination. The best performance was found at 8 nm thickness. Then, the model was used to simulate the work in the study [20] to evaluate its application possibility for real OSCs. For J_{sc} and V_{oc}, the result from simulation and experiment was quite similar. However, the FF and PCE from the 7 nm model were 2.13% and 0.12% higher, respectively. These differences are expected from the fixed ideality factor *n* in the simulation. Nevertheless, the simulation model still showed good results, compared to the experimental data and can work well with other actual OSCs.

LIST OF ABBREVIATIONS

P3HT = poly(3-hexylthiophene-2,5-diyl)
 PCBM = phenyl-C61 butyric acid methyl ester
 ZnO = Zinc Oxide
 J_{sc} = short circuit current density

FF = fill factor
 V_{oc} = open circuit voltage
 OSCs = Organic solar cells
 PCE = power conversion efficiency
 BLs = buffer layers
 BHJ = bulk heterojunction
 CBL = cathode buffer layer
 ETL = electron transport layer
 HBL = hole blocking layer

ETHICS APPROVAL AND CONSENT TO PARTICIPATE

Not applicable.

HUMAN AND ANIMAL RIGHTS

No Animals/Humans were used for studies that are the basis of this research.

CONSENT FOR PUBLICATION

Not applicable.

AVAILABILITY OF DATA AND MATERIALS

Not applicable.

FUNDING

This research is funded by Vietnam National University, Hanoi (VNU), under project number QG.19.20.

CONFLICT OF INTEREST

The authors declare no conflict of interest, financial or otherwise.

ACKNOWLEDGEMENTS

This research is funded by Vietnam National University, Hanoi (VNU) under project number QG.19.20.

REFERENCES

- [1] Dang, M.T.; Hirsch, L.; Wantz, G. P3HT:PCBM, best seller in polymer photovoltaic research. *Adv. Mater.*, **2011**, *23*(31), 3597-3602.
<http://dx.doi.org/10.1002/adma.201100792> PMID: 21936074
- [2] Abada, Z.; Mellit, A. Optical optimization of organic solar cells based on P3HT: PCBM interpenetrating blend. *2017 5th International Conference on Electrical Engineering - Boumerdes (ICEE-B)*, **2017**, pp. 29-31.
- [3] Ramirez, O.; Cabrera, V.; Reséndiz, L.M. Optimum ratio of electron-to-hole mobility in P3HT: PCBM organic solar cells. *Opt. Quantum Electron.*, **2014**, *46*, 1291-1296.
<http://dx.doi.org/10.1007/s11082-013-9855-1>
- [4] Kumar, P.; Jain, S.; Kumar, V.; Chand, S.; Tandon, R.P. A model for the J-V characteristics of P3HT: PCBM solar cells. *J. Appl. Phys.*, **2009**, *105*104507
<http://dx.doi.org/10.1063/1.3129320>
- [5] Moulé, A.J.; Bonekamp, J.B.; Meerholz, K. The effect of active layer thickness and composition on the performance of bulk-heterojunction solar cells. *J. Appl. Phys.*, **2006**, *100*094503
<http://dx.doi.org/10.1063/1.2360780>
- [6] Hoppe, H.; Sariciftci, N.S. Organic solar cells: An overview. *J. Mater. Res.*, **2004**, *19*, 1924-1945.
<http://dx.doi.org/10.1557/JMR.2004.0252>
- [7] Berger, P. Energy. Polymer solar cells: P3HT: PCBM and beyond. *J. Renew. Sustain. Energy*, **2018**, *100*13508
<http://dx.doi.org/10.1063/1.5012992>
- [8] Liang, Z.; Zhang, Q.; Jiang, L.; Cao, G. ZnO cathode buffer layers for inverted polymer solar cells. *Energy Environ. Sci.*, **2015**, *8*, 3442-3476.
<http://dx.doi.org/10.1039/C5EE02510A>
- [9] Lan, D.; Ming, Q.; Ruisheng, Y.; Hongjijing, W.; Zirui, J. Kai-chang, Kou, Guanglei, W.; Yuancheng, F.; Quanhong, F.; Fuli, Z. Synthesis, characterization and microwave transparent properties of Mn₃O₄ microspheres. *J. Mater. Sci. Mater. Electron.*, **2019**, *30*, 8771-8776.
<http://dx.doi.org/10.1007/s10854-019-01201-7>
- [10] Qin, M.; Lan, D.; Liu, J.; Liang, H.; Zhang, L.; Xing, H.; Xu, T.; Wu, H. Synthesis of single-component metal oxides with controllable multi-shelled structure and their morphology-related applications. *Chem. Rec.*, **2019**, *12*, 1-19.
<http://dx.doi.org/10.1002/tcr.201900017> PMID: 31250979
- [11] Huang, J.; Yin, Z.; Zheng, Q. Applications of ZnO in organic and hybrid solar cells. *Energy Environ. Sci.*, **2011**, *4*, 3861-3877.
<http://dx.doi.org/10.1039/c1ee01873f>
- [12] Nguyen, N.D.; Kim, H.K.; Nguyen, D.L.; Nguyen, D.C.; Nguyen, P.H.N. Characterization of performance parameters of organic solar cells with a buffer ZnO layer. *Adv. Nat. Sci. Nanosci. Nanotechnol.*, **2019**, *100*15005
<http://dx.doi.org/10.1088/2043-6254/aafda1>
- [13] Kirchartz, T.; Agostinelli, T.; Campoy-Quiles, M.; Gong, W.; Nelson, J. Understanding the thickness-dependent performance of organic bulk heterojunction solar cells: The influence of mobility, lifetime, and space charge. *J. Phys. Chem. Lett.*, **2012**, *3*(23), 3470-3475.
<http://dx.doi.org/10.1021/jz301639y> PMID: 26290974
- [14] Movla, H.; Shahalizad, A.; Abad, A.R.N. Influence of active region thickness on the performance of bulk heterojunction solar cells: Electrical modeling and simulation. *Opt. Quantum Electron.*, **2015**, *47*, 621-632.
<http://dx.doi.org/10.1007/s11082-014-9938-7>
- [15] Ompong, D.; Singh, J. Charge carrier mobility dependent open circuit voltage in organic and hybrid solar cells. *Front. Nanosci. Nanotech.*, **2016**, *2*, 43-47.
<http://dx.doi.org/10.15761/FNN.1000108>
- [16] Takanezawa, K.; Hirota, K.; Wei, Q.S.; Tajima, K.; Hashimoto, K. Efficient charge collection with ZnO nanorod array in hybrid photovoltaic devices. *J. Phys. Chem. C*, **2007**, *111*, 7218-7223.
<http://dx.doi.org/10.1021/jp071418n>
- [17] Chi, D.; Shihua, H.; Shizhong, Y.; Kong, L.; Shudi, L.; Zhije, W.; Shengchun, Q.; Zhanguo, W. Ultra-thin ZnO film as an electron transport layer for realizing the high efficiency of organic solar cells. *RCS Adv.*, **2017**, *7*, 14694-14700.
<http://dx.doi.org/10.1039/C6RA27543E>
- [18] Karim, M.R.; Shar, M.A.; Abdullah, S. Mixed dyes for dye-sensitized solar cells applications. *Curr. Nanosci.*, **2019**, *15*, 501-505.
<http://dx.doi.org/10.2174/1573413715666190325165613>
- [19] Kim, J.Y.; Hyunkoo, L.; Jungho, P.; Donggu, L.; Hyung-Jun, S.; Jeonghun, K.; Changhee, L. Effect of sol-gel-derived ZnO interfacial layer on the photovoltaic properties of polymer solar cells. *Jpn. J. Appl. Phys.*, **2012**, *51*10NE29
<http://dx.doi.org/10.7567/JJAP.51.10NE29>
- [20] Liang, Z.; Zhang, Q.; Orawan, W.; Junting, X.; Yang, Z.; Kwangsuk, P. Chundong, L.; Guozhong, C. Effects of the morphology of a ZnO buffer layer on the photovoltaic performance of inverted polymer solar cells. *Adv. Funct. Mater.*, **2012**, *22*, 2194-2201.
<http://dx.doi.org/10.1002/adfm.201101915>
- [21] Vanlaeke, P.; Swinnen, A.; Haeldermans, I.; Vanhoyland, G.; Aernouts, T.; Cheyns, D.; Deibel, C.; D'Haen, J.; Heremans, P.; Poortmans, J.; Manca, J.V. P3HT/PCBM bulk heterojunction solar cells: Relation between morphology and electro-optical characteristics. *Sol. Energy Mater. Sol. Cells*, **2006**, *90*, 2150-2158.
<http://dx.doi.org/10.1016/j.solmat.2006.02.010>